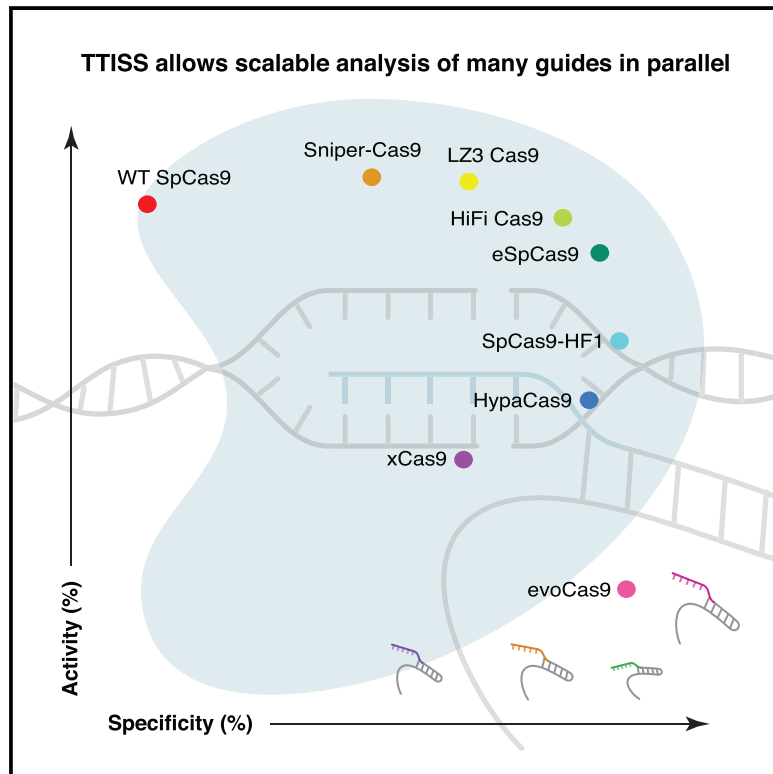# Molecular Cell

Highly Parallel Profiling of Cas9 Variant Specificity

Graphical Abstract

Authors

Jonathan L. Schmid-Burgk, Linyi Gao, David Li, Zachary Gardner, Jonathan Strecker, Blake Lash, Feng Zhang

Correspondence

zhang@broadinstitute.org

In Brief

Schmid-Burgk et al. develop tagmentation-based tag integration site sequencing (TTISS), a rapid, streamlined protocol for analyzing double-strand breaks such as those created by CRISPR nucleases. Using TTISS, they comprehensively assess Cas9 variants, revealing a trade-off between specificity and activity and identifying LZ3 Cas9, a variant with a unique +1 insertion profile.

Highlights

- Tagmentation-based tag integration site sequencing (TTISS) scalably detects DSBs

- TTISS is a rapid and streamlined protocol compatible with multiplexing

- Application of TTISS highlights trade-off in Cas9 variant specificity and activity

- LZ3 Cas9 variant exhibits a unique +1 insertion profile

CellPress

Molecular Cell

Technology

CellPress

Highly Parallel Profiling of Cas9 Variant Specificity

Jonathan L. Schmid-Burgk,[1,2,3,4,6] Linyi Gao,[1,2,3,4,6] David Li,[1,2,3,4,6] Zachary Gardner,[1,2,3,4] Jonathan Strecker,[1,2,3,4] Blake Lash,[1,2,3,4] and Feng Zhang[1,2,3,4,5,6,7,*]

[1]Broad Institute of MIT and Harvard, Cambridge, MA 02142, USA
[2]McGovern Institute for Brain Research, Massachusetts Institute of Technology, Cambridge, MA 02139, USA
[3]Department of Brain and Cognitive Sciences, Massachusetts Institute of Technology, Cambridge, MA 02139, USA
[4]Department of Biological Engineering, Massachusetts Institute of Technology, Cambridge, MA 02139, USA
[5]Howard Hughes Medical Institute, Cambridge, MA 02139, USA
[6]These authors contributed equally
[7]Lead Contact
*Correspondence: zhang@broadinstitute.org
https://doi.org/10.1016/j.molcel.2020.02.023

SUMMARY

Determining the off-target cleavage profile of programmable nucleases is an important consideration for any genome editing experiment, and a number of Cas9 variants have been reported that improve specificity. We describe here tagmentation-based tag integration site sequencing (TTISS), an efficient, scalable method for analyzing double-strand breaks (DSBs) that we apply in parallel to eight Cas9 variants across 59 targets. Additionally, we generated thousands of other Cas9 variants and screened for variants with enhanced specificity and activity, identifying LZ3 Cas9, a high specificity variant with a unique +1 insertion profile. This comprehensive comparison reveals a general trade-off between Cas9 activity and specificity and provides information about the frequency of generation of +1 insertions, which has implications for correcting frameshift mutations.

INTRODUCTION

CRISPR-Cas9 technology is widely used for genome editing and is currently being tested in clinical trials as a therapeutic. Many applications of this technology rely on Cas9 from *Streptococcus pyogenes* (SpCas9), and a number of engineered or evolved SpCas9 variants have been reported that impact Cas9 specificity. It is known that Cas9 activity and editing outcome vary depending on both the protein and the guide RNA, and thus empirically determining optimal enzyme-guide combinations may be helpful, particularly for clinical applications. Although a number of techniques have been developed that assess off-target cleavage (Tsai and Joung, 2016), these techniques are relatively low-throughput—limited to one guide per barcoded sample. We therefore developed tagmentation-based tag integration site sequencing (TTISS), an efficient, rapid, scalable method to assess editing outcomes.

DESIGN

Our method builds on the genome-wide, unbiased identification of double-strand breaks (DSBs) enabled by sequencing (GUIDE-seq) (Tsai et al., 2015) approach of tagging DSBs induced by nuclease cleavage through integration of a double-stranded donor DNA, but makes use of guide multiplexing and bulk tagmentation by Tn5 (Picelli et al., 2014), which can be performed directly in lysed cells, leading to an efficient, rapid protocol (Figure 1A). Following tagmentation, DNA is quickly purified using a spin column. Integration sites are enriched using two nested PCRs, which provide sufficient specificity to allow direct sequencing of the final product without further enrichment. Assigning the sequenced integration sites to guides by sequence similarity generates a list of off-target sites for each guide in parallel.

RESULTS

The sensitivity of TTISS is comparable to GUIDE-seq (Table S1, note GUIDE-seq data are from U-2 OS cells using matched single guides) and discovery of *in situ* Cas off-targets and verification by sequencing (DISCOVER-seq) (Table S1, using matched single guides) (Wienert et al., 2019). TTISS is scalable to at least 60 guides per transfection in HEK293T cells (Figure S1A), while retaining 71.4% of off-target sites detected in a single guide experiment, and is compatible with multiple cell types (Figure S1B). Additionally, TTISS can be extended to profiling of prime editing-mediated donor integration (Anzalone et al., 2019), which showed no off-target integration events for three integration sites tested (Figure S1C).

We used TTISS to assess the specificity of wild-type (WT) SpCas9 and eight SpCas9 specificity variants—eSpCas9(1.1) (Slaymaker et al., 2016), SpCas9-HF1 (Kleinstiver et al., 2016), HypaCas9 (Chen et al., 2017), evoCas9 (Casini et al., 2018), xCas9(3.7) (Hu et al., 2018), Sniper-Cas9 (Lee et al., 2018), HiFi Cas9 (Vakulskas et al., 2018)—and one newly generated specificity variant, LZ3 Cas9 (Figure 2; STAR Methods) in parallel using 59 guides in two pools randomly selected from the genome-scale CRISPR knock out (GeCKO) library (Shalem et al., 2014) that all start with a guanine to improve U6 transcription
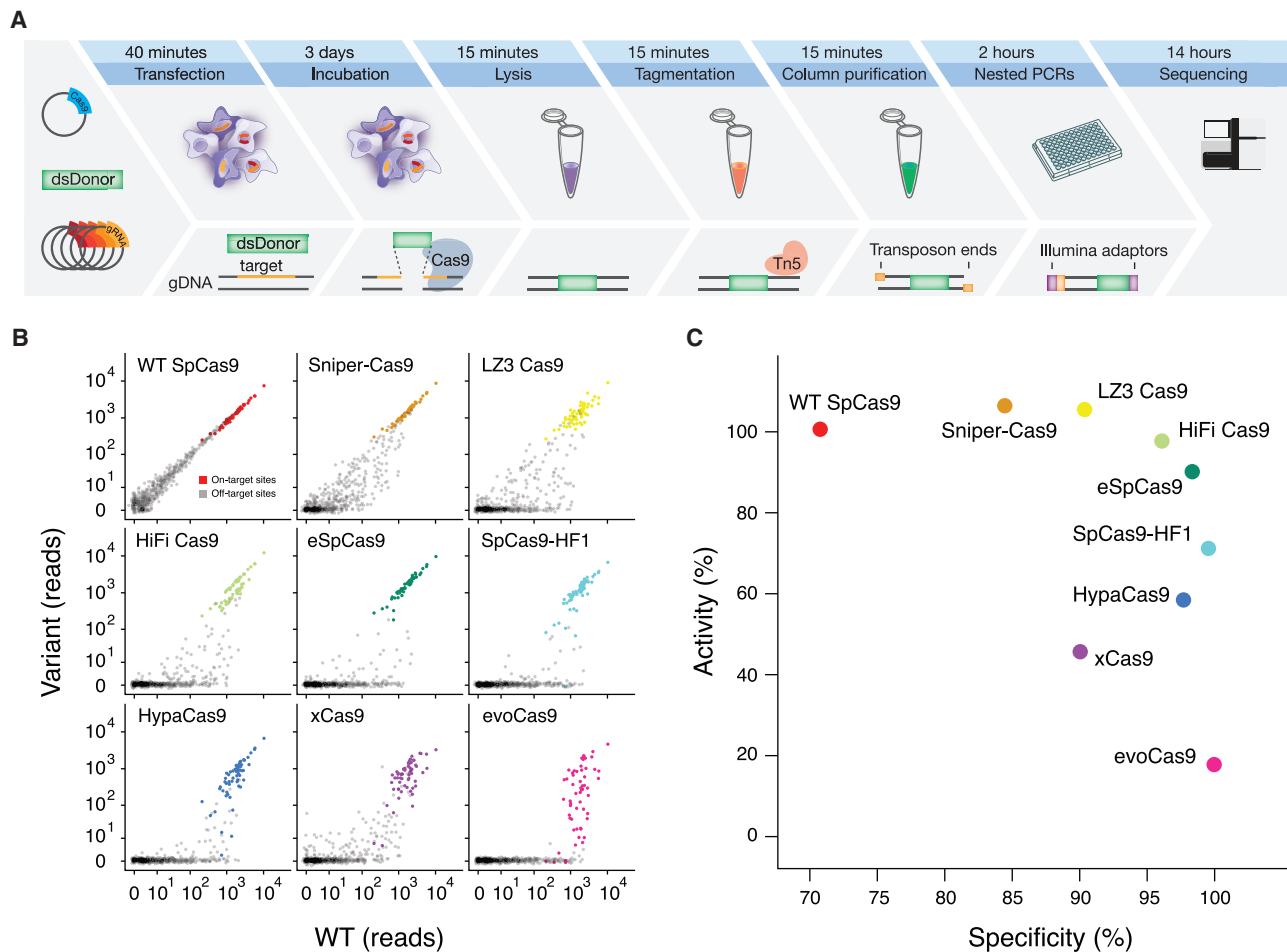
Figure 1. TTISS Allows Multiplexed Assessment of Nuclease Off-Targets
(A) Schematic of TTISS off-target detection method.
(B) TTISS results for 59 guides from the GeCKO library tested across eight SpCas9 specificity variants and WT SpCas9.
(C) Specificity and activity scores for all tested SpCas9 variants.
See also Figures S1 and S2 and Tables S1, S2, and S3.

(Figure 1B). For WT SpCas9, TTISS detected 607 total off-target sites across two technical replicates, with individual guides contributing 0–225 off-target sites (Figure S1D; Table S2). Although each specificity variant showed improvement relative to WT SpCas9, a systematic comparison of these variants has not been reported. Using TTISS, we found that, although each specificity variant eliminated at least half of the WT SpCas9 off-targets, there was a wide range of specificities among variants, with evoCas9 being most specific (4 detected off-targets) and SniperCas9 being least specific (287 detected off-targets) (Figure 1B).

Measuring on-target indel frequencies by targeted sequencing revealed that evoCas9 and xCas9(3.7) have the lowest on-target activity, while LZ3 Cas9, HiFi Cas9, and Sniper-Cas9 have on-target activity comparable to WT SpCas9 (Figures S2A and S2B). To compare specificity variants more broadly, we calculated an activity and a specificity score for each variant (Figure 1C), revealing a general trade-off between activity and specificity among all variants.

To assess whether this observed trade-off between activity and specificity is a general feature of the SpCas9 mutation space, we performed a high-throughput pooled lentiviral screen to comprehensively profile variant activity in human cells. We selected 157 residues for mutagenesis (Figure 2A), focusing on the HNH and RuvC nuclease domains, as well as the L1 and L2 linkers connecting them, as these regions play a key role in the conformational activation of Cas9 to license target cleavage (Palermo et al., 2016). We selected four diverse target sites to assay the variants on: a putative "permissive" guide (g1) known to be highly active for eSpCas9(1.1) and SpCas9-HF1; a "difficult" guide (g2) with no activity for eSpCas9(1.1) and SpCas9-HF1; and two simulated off-targets (g3 and g4) bearing two mismatches each (Figure 2B). Barcoded variants were cloned into a lentiviral vector and transduced into HEK293FT cells (Figure 2C), along with a guide RNA cassette and cognate target site. A total of 2,420 single amino acid variants exceeded the minimum read threshold for all four targets, representing 9.2% of all possible single amino acid variants of SpCas9. The
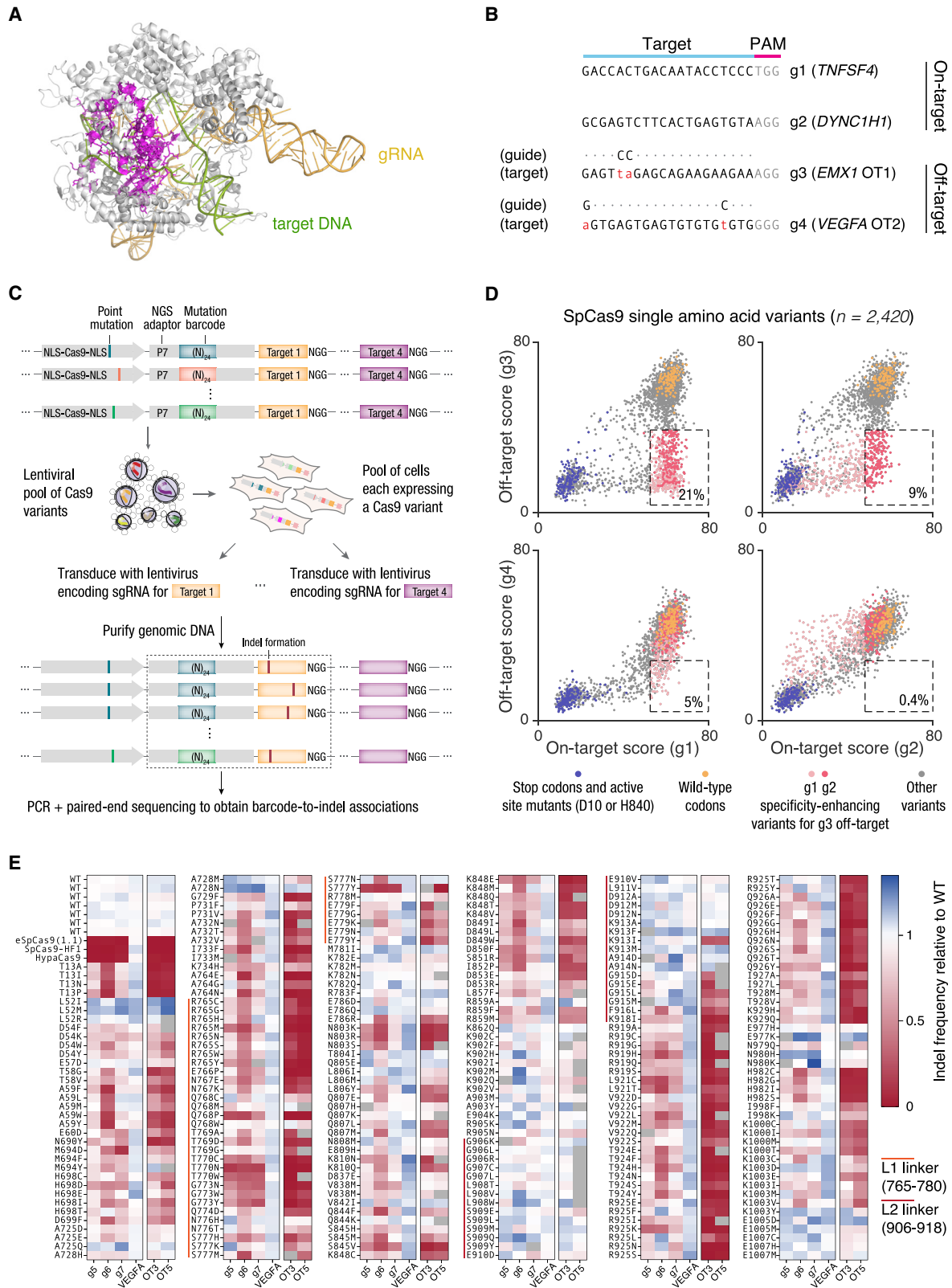
(legend on next page)

activity of these variants was highly guide-dependent: over 20% of the variants improved specificity ($\leq$50% activity at mismatched off-target; $\geq$80% activity on-target) when comparing g1 versus g3, while <1% of variants met these criteria when comparing g2 versus g4 (Figure 2D). We validated the performance of 254 variants on a broader range of targets (including three targets known to have low activity for eSpCas9(1.1) and SpCas9-HF1) by individual transfections and targeted deep sequencing (Figure 2E). Overall, these results suggest that a simple guide-dependent trade-off describes the performance of a broad range of Cas9 variants.

A number of algorithms have been developed that aim to predict editing outcomes, including specificity and, more recently, indel distributions. Comparison of TTISS specificity data to two published computational tools that provide specificity scores for guides—GuideScan (https://guidescan.com) (Perez et al., 2017) and CRISPR ML (https://crispr.ml) (Listgarten et al., 2018) showed a weak correlation (GuideScan, n = 59, R = 0.408, CRISPR ML, n = 47, R = 0.111) between the predicted metric and empirical observation (Figures S1E and S1F).

Although the predominant outcome of Cas9 cleavage is a blunt DSB created by the concerted effort of the two nuclease domains, HNH and RuvC, the RuvC domain is not as rigidly positioned, and it can slide one base upstream (distal to the PAM), giving rise to a staggered cut that is filled in by the cellular repair machinery and leads to duplication of a single base (+1 insertion) (Figure 3A) (Zuo and Liu, 2016). This property is particularly useful in the genome engineering context because +1 insertions in protein-coding regions guarantee frameshifts, which has utility either for knocking out a gene or for the correction of a genetic variant. We therefore examined whether we could predict the relative frequencies of +1 insertions in the indel distribution for a given on-target site from multiplex TTISS data. Because TTISS relies on integration of a donor, we cannot directly observe +1 insertions, so we developed an algorithm to predict +1 insertions based on the distribution of the position of the donor relative to the cut site. To obtain the distribution for each cut site, we compiled the number of donor integrations at each nucleotide position relative to the cut site for both ends of the donor. We then used a convolution operation to merge these two distributions to model the situation in which no donor is integrated, allowing us to predict +1 frequencies (Figure 3B). To validate our approach, we compared the +1 frequencies obtained by TTISS for WT SpCas9 for 58 guides to those measured by targeted indel sequencing (Figure S3A) and found a high correlation (r = 0.829), suggesting TTISS can be used to predict +1 frequency of a given guide. Prediction tools for Cas9-induced indel length distributions performed heteroge-

neously in predicting +1 frequencies compared to our empirical data (FORECasT [Allen et al., 2018], R = 0.782; inDelphi [Shen et al., 2018], R = −0.075; Lindel [Chen et al., 2019], R = 0.839) (Figure S3A).

Given that many of the Cas9 variants contain mutations impacting DNA binding, which could potentially affect RuvC positioning, we compared the indel patterns of Cas9 specificity variants across a set of 58 guides. While most variants closely mirrored +1 frequencies of WT SpCas9 across on-target sites by TTISS (Figure S3B), the variant LZ3 Cas9 exhibited a markedly different +1 frequency profile relative to WT SpCas9 (Figure 3C), which was confirmed by targeted sequencing data (Figure S3D). Exploring sequence determinants for +1 frequencies of LZ3 Cas9 and WT SpCas9 revealed that for both enzymes, the presence of a thymidine or a guanine in the −4 position with respect to the PAM led to the highest and lowest rates of +1 insertion respectively (Figure S3C). However, when comparing LZ3 Cas9 to WT SpCas9, LZ3 Cas9 showed elevated +1 frequency given a guanine at position −2 (Figure 3D). In contrast, overall indel profiles were not found to be altered for any of the Cas9 variants tested (Figure S3E).

DISCUSSION

Here, we have shown that TTISS is a scalable, accessible, and cost-effective method for examining off-targets and +1 insertion frequencies of programmable nucleases. Beyond these applications, TTISS has been successfully applied to detect off-targets in other genome editing contexts, including editing by Cas enzymes creating overhanging, rather than blunt, ends (Strecker et al., 2019a), Cas enzymes delivered as ribonucleoprotein complexes, and ShCAST-mediated genome insertions (Strecker et al., 2019b). Multiplex TTISS enables the creation of substantially larger sets of empirical data that could contribute to improved predictive algorithms or identify high-specificity guides suitable for clinical applications. Applying TTISS across a panel of SpCas9 variants revealed a tradeoff between activity and specificity, which is also supported by our Cas9 mutational screening results. We also showed that the newly evolved LZ3 Cas9 variant exhibits high activity, increased specificity, and a differential +1 insertion profile as compared to WT SpCas9. Further rational engineering of LZ3 Cas9 might provide an avenue for non-templated correction of disease-causing frameshift mutations in the human population.

Limitations

Among published off-target detection methods, TTISS requires the least hands-on time with very few enzymatic steps and is

Figure 2. High-Throughput Profiling of SpCas9 Mutant Fitness in Human Cells
(A) Crystal structure of SpCas9 (PDB: 5F9R) showing the positions of 157 residues (magenta) selected for mutagenesis.
(B) Sequences of target sites used for screening.
(C) Approach for pooled lentiviral screening of SpCas9 variants in HEK293FT cells.
(D) Scatterplots of on-target versus off-target activity scores for 2,420 SpCas9 single amino acid variants. The dashed box in each subplot contains all variants with $\geq$80% of the median WT on-target activity and $\leq$50% of the median WT off-target activity; activities were calculated after subtracting the median background activity of stop codon variants. The percentage within each box represents the percentage of all variants that lie within the box.
(E) On-target and off-target activity of 254 SpCas9 single amino acid variants, quantified by targeted deep sequencing of individually transfected constructs. See also Figure S2.
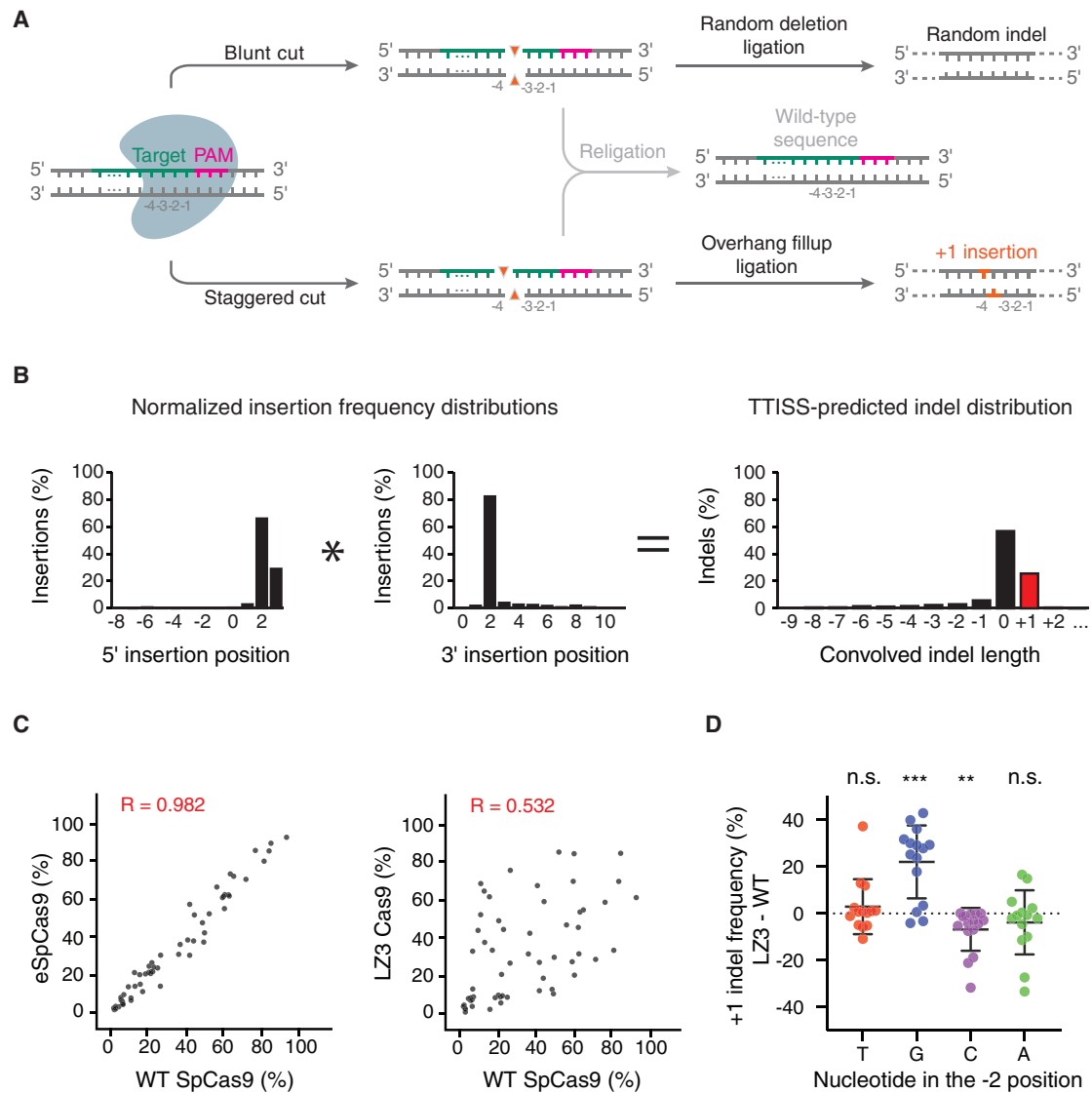
Figure 3. Multiplexed Assessment of +1 Indel Frequencies Using TTISS

(A) Editing outcomes of nuclease-induced blunt or staggered cuts in the human genome. As a simplified model, blunt or staggered cuts can either be resected prior to re-ligation, creating random deletions (top panel) or re-ligated without resection (middle panel). Staggered 5′ overhangs can be filled in before re-ligation, causing duplication of base −4 respective to the PAM motif (bottom panel).

(B) Schematic for convolution operation used to predict indel distributions by TTISS.

(C) Representative examples of TTISS-predicted +1 insertion frequencies compared between specificity variants versus WT SpCas9 for 58 gRNAs.

(D) Differential +1 indel frequencies between LZ3 Cas9 and WT SpCas9 +1 insertion frequencies from targeted indel sequencing, grouped by the nucleotide identity at the −2 position relative to the PAM. Bars represent mean +/- standard deviation. Results from two-tailed t test for significant divergence from zero are indicated by **p < 0.01 and ***p < 0.001; n.s., not significant.

See also Figure S3.

the only method demonstrated to be compatible with multiplexing >50 guides in a single experiment. For instances where *in vitro* rather than *in vivo* specificity profiles are desired, Digenome-seq, circularization for in vitro reporting of cleavage effects by sequencing (CIRCLE-seq), or selective enrichment and identification of adapter-tagged DNA ends by sequencing (SITE-seq) should be used (Cameron et al., 2017; Kim et al., 2015; Tsai et al., 2017), all of which can potentially be adapted to guide multiplexing using our analysis pipeline. Whereas GUIDE-seq and TTISS capture relevant *in vivo* biases from cleavage and non-homologous end joining (NHEJ) repair processes, DISCOVER-seq instead captures binding of the MRN repair complex, adding potentially relevant information for assessing the safety of Cas enzymes (and other programmable nucleases) for clinical application (Wienert et al., 2019).

CellPress

STAR★METHODS

Detailed methods are provided in the online version of this paper and include the following:

- KEY RESOURCES TABLE
- LEAD CONTACT AND MATERIALS AVAILABILITY
- EXPERIMENTAL MODEL AND SUBJECT DETAILS
  - HEK293T cells
  - U-2 OS cells
  - K562 cells
  - *E. coli* strains
- METHOD DETAILS
  - Tn5 purification
  - Tn5 loading with single handle
  - Cas9 variant cloning
  - Cell transfection
  - Cell lysis and genome tagmentation
  - PCR amplification
  - Deep sequencing
  - Read mapping
  - Integration site detection
  - gRNA assignment
  - Prediction of indel length distributions
  - Variant Scoring
  - Cas9 variant library construction
  - Lentiviral Cas9 variant library screen
  - Cas9 variant validation and combinatorial mutagenesis
  - Prime editing constructs
  - Targeted indel sequencing
  - Indel distribution and specificity predictors
- QUANTIFICATION AND STATISTICAL ANALYSIS
- DATA AND CODE AVAILABILITY
- ADDITIONAL RESOURCES
  - Detailed protocol
  - Bench Protocol

SUPPLEMENTAL INFORMATION

Supplemental Information can be found online at https://doi.org/10.1016/j.molcel.2020.02.023.

AUTHOR CONTRIBUTIONS

J.L.S.-B., L.G., D.L., and F.Z. designed the experiments. L.G., D.L., J.L.S.-B., Z.G., J.S., and B.L. collected the data. D.L., L.G., J.L.S.-B., and B.L. analyzed the data. J.L.S.-B., L.G., D.L., and F.Z. wrote the manuscript with input from all coauthors.

REFERENCES

Allen, F., Crepaldi, L., Alsinet, C., Strong, A.J., Kleshchevnikov, V., De Angeli, P., Páleníková, P., Khodak, A., Kiselev, V., Kosicki, M., et al. (2018). Predicting the mutations generated by repair of Cas9-induced double-strand breaks. Nat. Biotechnol. *37*, 64–72.

Anzalone, A.V., Randolph, P.B., Davis, J.R., Sousa, A.A., Koblan, L.W., Levy, J.M., Chen, P.J., Wilson, C., Newby, G.A., Raguram, A., and Liu, D.R. (2019). Search-and-replace genome editing without double-strand breaks or donor DNA. Nature *576*, 149–157.

Cameron, P., Fuller, C.K., Donohoue, P.D., Jones, B.N., Thompson, M.S., Carter, M.M., Gradia, S., Vidal, B., Garner, E., Slorach, E.M., et al. (2017). Mapping the genomic landscape of CRISPR-Cas9 cleavage. Nat. Methods *14*, 600–606.

Casini, A., Olivieri, M., Petris, G., Montagna, C., Reginato, G., Maule, G., Lorenzin, F., Prandi, D., Romanel, A., Demichelis, F., et al. (2018). A highly specific SpCas9 variant is identified by in vivo screening in yeast. Nat. Biotechnol. *36*, 265–271.

Chen, J.S., Dagdas, Y.S., Kleinstiver, B.P., Welch, M.M., Sousa, A.A., Harrington, L.B., Sternberg, S.H., Joung, J.K., Yildiz, A., and Doudna, J.A. (2017). Enhanced proofreading governs CRISPR-Cas9 targeting accuracy. Nature *550*, 407–410.

Chen, W., McKenna, A., Schreiber, J., Haeussler, M., Yin, Y., Agarwal, V., Noble, W.S., and Shendure, J. (2019). Massively parallel profiling and predictive modeling of the outcomes of CRISPR/Cas9-mediated double-strand break repair. Nucleic Acids Res. *47*, 7989–8003.

Gao, L., Cox, D.B.T., Yan, W.X., Manteiga, J.C., Schneider, M.W., Yamano, T., Nishimasu, H., Nureki, O., Crosetto, N., and Zhang, F. (2017). Engineered Cpf1 variants with altered PAM specificities. Nat. Biotechnol. *35*, 789–792.

Hu, J.H., Miller, S.M., Geurts, M.H., Tang, W., Chen, L., Sun, N., Zeina, C.M., Gao, X., Rees, H.A., Lin, Z., and Liu, D.R. (2018). Evolved Cas9 variants with broad PAM compatibility and high DNA specificity. Nature *556*, 57–63.

Kim, D., Bae, S., Park, J., Kim, E., Kim, S., Yu, H.R., Hwang, J., Kim, J.-I., and Kim, J.-S. (2015). Digenome-seq: genome-wide profiling of CRISPR-Cas9 off-target effects in human cells. Nat. Methods *12*, 237–243, 1, 243.

Kleinstiver, B.P., Pattanayak, V., Prew, M.S., Tsai, S.Q., Nguyen, N.T., Zheng, Z., and Joung, J.K. (2016). High-fidelity CRISPR-Cas9 nucleases with no detectable genome-wide off-target effects. Nature *529*, 490–495.

Lee, J.K., Jeong, E., Lee, J., Jung, M., Shin, E., Kim, Y.-H., Lee, K., Jung, I., Kim, D., Kim, S., and Kim, J.S. (2018). Directed evolution of CRISPR-Cas9 to increase its specificity. Nat. Commun. *9*, 3048.

Listgarten, J., Weinstein, M., Kleinstiver, B.P., Sousa, A.A., Joung, J.K., Crawford, J., Gao, K., Hoang, L., Elibol, M., Doench, J.G., and Fusi, N. (2018). Prediction of off-target activities for the end-to-end design of CRISPR guide RNAs. Nat. Biomed. Eng. *2*, 38–47.

Palermo, G., Miao, Y., Walker, R.C., Jinek, M., and McCammon, J.A. (2016). Striking Plasticity of CRISPR-Cas9 and Key Role of Non-target DNA, as Revealed by Molecular Simulations. ACS Cent. Sci. *2*, 756–763.

Perez, A.R., Pritykin, Y., Vidigal, J.A., Chhangawala, S., Zamparo, L., Leslie, C.S., and Ventura, A. (2017). GuideScan software for improved single and paired CRISPR guide RNA design. Nat. Biotechnol. 35, 347–349.

Picelli, S., Björklund, A.K., Reinius, B., Sagasser, S., Winberg, G., and Sandberg, R. (2014). Tn5 transposase and tagmentation procedures for massively scaled sequencing projects. Genome Res. 24, 2033–2040.

Ran, F.A., Hsu, P.D., Wright, J., Agarwala, V., Scott, D.A., and Zhang, F. (2013). Genome engineering using the CRISPR-Cas9 system. Nat. Protoc. 8, 2281–2308.

Schmid-Burgk, J.L., and Hornung, V. (2015). BrowserGenome.org: web-based RNA-seq data analysis and visualization. Nat. Methods 12, 1001.

Schmid-Burgk, J.L., Schmidt, T., Gaidt, M.M., Pelka, K., Latz, E., Ebert, T.S., and Hornung, V. (2014). OutKnocker: a web tool for rapid and simple genotyping of designer nuclease edited cell lines. Genome Res. 24, 1719–1723.

Shalem, O., Sanjana, N.E., Hartenian, E., Shi, X., Scott, D.A., Mikkelson, T., Heckl, D., Ebert, B.L., Root, D.E., Doench, J.G., and Zhang, F. (2014). Genome-scale CRISPR-Cas9 knockout screening in human cells. Science 343, 84–87.

Shen, M.W., Arbab, M., Hsu, J.Y., Worstell, D., Culbertson, S.J., Krabbe, O., Cassa, C.A., Liu, D.R., Gifford, D.K., and Sherwood, R.I. (2018). Predictable and precise template-free CRISPR editing of pathogenic variants. Nature 563, 646–651.

Slaymaker, I.M., Gao, L., Zetsche, B., Scott, D.A., Yan, W.X., and Zhang, F. (2016). Rationally engineered Cas9 nucleases with improved specificity. Science 351, 84–88.

Strecker, J., Jones, S., Koopal, B., Schmid-Burgk, J., Zetsche, B., Gao, L., Makarova, K.S., Koonin, E.V., and Zhang, F. (2019a). Engineering of CRISPR-Cas12b for human genome editing. Nat. Commun. 10, 212.

Strecker, J., Ladha, A., Gardner, Z., Schmid-Burgk, J.L., Makarova, K.S., Koonin, E.V., and Zhang, F. (2019b). RNA-guided DNA insertion with CRISPR-associated transposases. Science 365, 48–53.

Tsai, S.Q., and Joung, J.K. (2016). Defining and improving the genome-wide specificities of CRISPR-Cas9 nucleases. Nat. Rev. Genet. 17, 300–312.

Tsai, S.Q., Zheng, Z., Nguyen, N.T., Liebers, M., Topkar, V.V., Thapar, V., Wyvekens, N., Khayter, C., Iafrate, A.J., Le, L.P., et al. (2015). GUIDE-seq enables genome-wide profiling of off-target cleavage by CRISPR-Cas nucleases. Nat. Biotechnol. 33, 187–197.

Tsai, S.Q., Nguyen, N.T., Malagon-Lopez, J., Topkar, V.V., Aryee, M.J., and Joung, J.K. (2017). CIRCLE-seq: a highly sensitive in vitro screen for genome-wide CRISPR-Cas9 nuclease off-targets. Nat. Methods 14, 607–614.

Vakulskas, C.A., Dever, D.P., Rettig, G.R., Turk, R., Jacobi, A.M., Collingwood, M.A., Bode, N.M., McNeill, M.S., Yan, S., Camarena, J., et al. (2018). A high-fidelity Cas9 mutant delivered as a ribonucleoprotein complex enables efficient gene editing in human hematopoietic stem and progenitor cells. Nat. Med. 24, 1216–1224.

Wienert, B., Wyman, S.K., Richardson, C.D., Yeh, C.D., Akcakaya, P., Porritt, M.J., Morlock, M., Vu, J.T., Kazane, K.R., Watry, H.L., et al. (2019). Unbiased detection of CRISPR off-targets in vivo using DISCOVER-Seq. Science 364, 286–289.

Zuo, Z., and Liu, J. (2016). Cas9-catalyzed DNA Cleavage Generates Staggered Ends: Evidence from Molecular Dynamics Simulations. Sci. Rep. 5, 37584.

STAR★METHODS

KEY RESOURCES TABLE

REAGENT or RESOURCE	SOURCE	IDENTIFIER
Bacterial Strains		
STBL3	ThermoFisher	C737303
T7 Express *lysY/I^q* Competent *E. coli* (High Efficiency)	NEB	C3013
Chemicals, Peptides, and Recombinant Proteins		
FBS, USA, Seradigm Premium	VWR	97068-085
KOD Hot Start DNA Polymerase	Millipore Sigma	71086-3
Proteinase K	NEB	P8107S
Tn5	F. Zhang Lab	N/A
Qiaprep spin miniprep kit	QIAGEN	27106
IPTG	Millipore Sigma	I6758
cOmplete protease inhibitor	Millipore Sigma	11697498001
Benzonase	Millipore Sigma	E1014-25KU
Chitin resin	NEB	S6651L
OptiMEM	ThermoFisher	31985070
E-Gel EX Agarose Gels, 2%	ThermoFisher	G402002
GeneJuice	Millipore Sigma	70967-3
SF Cell Line 4D-Nucleofector® X Kit	Lonza	V4XC-2012
SE. Cell Line 4D-Nucleofector® X Kit	Lonza	V4XC-1012
Puromycin	ThermoFisher	A1113802
NextSeq 500/550 High Output Kit v2, 75 cycles	Illumina	FC-404-2005
NextSeq 500/550 High Output Kit v2, 150 cycles	Illumina	FC-404-2002
Nuclease-Free Duplex Buffer	IDT	11-01-03-01
Deposited Data		
Deep Sequencing data	SRA	SRA: PRJNA602092
Experimental Models: Cell Lines		
HEK293T	Gift from Veit Hornung	N/A
U-2 OS	ATCC	HTB-96
K562	Millipore Sigma	89121407-1VL
Oligonucleotides		
/5Phos/CTGTCTCTTATACA/3ddC/	IDT	Transposon ME
GTCTCGTGGGCTCGGAGATGTGTATAAGAGACAG	IDT	Transposon read 2
/5phos/G*T*TGTGAGCAAGGGCGAGGAGGATAACGCCTCTCTCCCAGCGACT*A*T	IDT	TTISS donor sense
/5phos/A*T*AGTCGCTGGGAGAGAGGCGTTATCCTCCTCGCCCTTGCTCACA*A*C	IDT	TTISS donor antisense
GTCGCTGGGAGAGAGGCGTTATC	IDT	TTISS PCR fwd 1
AATGATACGGCGACCACCGAGATCTACACTATAGCCTACACTCTTTCCCTACACGACGCTCTTCCGATCTTTATCCTCCTCGCCCTTGCTCAC	IDT	TTISS PCR fwd 2
CAAGCAGAAGACGGCATACGAGATCGAGTAATGTCTCGTGGGCTCGGAGATGTGT	IDT	TTISS PCR rev BC1
CAAGCAGAAGACGGCATACGAGATTCTCCGGAGTCTCGTGGGCTCGGAGATGTGT	IDT	TTISS PCR rev BC2

Continued

REAGENT or RESOURCE	SOURCE	IDENTIFIER
CAAGCAGAAGACGGCATACGAGATAATGAGCGGTCTCGTGGGCTCGGAGATGTGT	IDT	TTISS PCR rev BC3
CAAGCAGAAGACGGCATACGAGATGGAATCTCGTCTCGTGGGCTCGGAGATGTGT	IDT	TTISS PCR rev BC4
CAAGCAGAAGACGGCATACGAGATTTCTGAATGTCTCGTGGGCTCGGAGATGTGT	IDT	TTISS PCR rev BC5
CAAGCAGAAGACGGCATACGAGATACGAATTCGTCTCGTGGGCTCGGAGATGTGT	IDT	TTISS PCR rev BC6
CAAGCAGAAGACGGCATACGAGATAGCTTCAGGTCTCGTGGGCTCGGAGATGTGT	IDT	TTISS PCR rev BC7
CAAGCAGAAGACGGCATACGAGATGCGCATTAGTCTCGTGGGCTCGGAGATGTGT	IDT	TTISS PCR rev BC8
CAAGCAGAAGACGGCATACGAGATCATAGCCGGTCTCGTGGGCTCGGAGATGTGT	IDT	TTISS PCR rev BC9
CAAGCAGAAGACGGCATACGAGATTTCGCGGAGTCTCGTGGGCTCGGAGATGTGT	IDT	TTISS PCR rev BC10
CAAGCAGAAGACGGCATACGAGATGCGCGAGAGTCTCGTGGGCTCGGAGATGTGT	IDT	TTISS PCR rev BC11
CAAGCAGAAGACGGCATACGAGATCTATCGCTGTCTCGTGGGCTCGGAGATGTGT	IDT	TTISS PCR rev BC12
CAAGCAGAAGACGGCATACGAGATTGTAGTGCGTCTCGTGGGCTCGGAGATGTGT	IDT	TTISS PCR rev BC13
CAAGCAGAAGACGGCATACGAGATGCGTCGACGTCTCGTGGGCTCGGAGATGTGT	IDT	TTISS PCR rev BC14
CAAGCAGAAGACGGCATACGAGATGGTCTTCTGTCTCGTGGGCTCGGAGATGTGT	IDT	TTISS PCR rev BC15
CAAGCAGAAGACGGCATACGAGATAAATGTCCGTCTCGTGGGCTCGGAGATGTGT	IDT	TTISS PCR rev BC16
CAAGCAGAAGACGGCATACGAGATGTTGAAACGTCTCGTGGGCTCGGAGATGTGT	IDT	TTISS PCR rev BC17
CAAGCAGAAGACGGCATACGAGATTCTTTACGGTCTCGTGGGCTCGGAGATGTGT	IDT	TTISS PCR rev BC18
CAAGCAGAAGACGGCATACGAGATATGCCTGGGTCTCGTGGGCTCGGAGATGTGT	IDT	TTISS PCR rev BC19
CAAGCAGAAGACGGCATACGAGATCAATAAGGGTCTCGTGGGCTCGGAGATGTGT	IDT	TTISS PCR rev BC20
CAAGCAGAAGACGGCATACGAGATCGCCGTAAGTCTCGTGGGCTCGGAGATGTGT	IDT	TTISS PCR rev BC21
CAAGCAGAAGACGGCATACGAGATTAAGGCTTGTCTCGTGGGCTCGGAGATGTGT	IDT	TTISS PCR rev BC22
CAAGCAGAAGACGGCATACGAGATTTGCTGCCGTCTCGTGGGCTCGGAGATGTGT	IDT	TTISS PCR rev BC23
CAAGCAGAAGACGGCATACGAGATCTCAATGTGTCTCGTGGGCTCGGAGATGTGT	IDT	TTISS PCR rev BC24
AATGATACGGCGACCACCGAGATCTACACTATAGCCTACACTCTTTCCCTACACGACGCTTATCGTCGTCATCCTTGT	IDT	TTISS PCR prime +24 fwd a
AATGATACGGCGACCACCGAGATCTACACTATAGCCTACACTCTTTCCCTACACGACGGATTACAAGGATGACGACGA	IDT	TTISS PCR prime +24 fwd b
GGCTTGTCGACGACGGCGGTC	IDT	TTISS PCR prime +38 fwd a1

(Continued on next page)

Continued

REAGENT or RESOURCE	SOURCE	IDENTIFIER
AATGATACGGCGACCACCGAGATCTACACTATAGCCTACACTCTTTCCCTACACGACGGACGGCGGTCTCCGTCGTCAG	IDT	TTISS PCR prime +38 fwd a2
ATGATCCTGACGACGGAGACCG	IDT	TTISS PCR prime +38 fwd b1
AATGATACGGCGACCACCGAGATCTACACTATAGCCTACACTCTTTCCCTACACGACGGACGGAGACCGCCGTCGTCGA	IDT	TTISS PCR prime +38 fwd b2
Recombinant DNA		
pX165-LZ3 Cas9	Addgene	#140561
pX165-HiFi Cas9	Addgene	#140563
pX165-eSpCas9	Addgene	#140564
pX165-Cas9-HF1	Addgene	#140565
pX165-HypaCas9	Addgene	#140567
pX165-xCas9	Addgene	#140568
pX165-evoCas9	Addgene	#140569
pU6-pegRNA-HEK3+24	Addgene	#140577
pU6-pegRNA-DNMT1+38	Addgene	#140578
pU6-pegRNA-EMX1+38	Addgene	#140579
pmCherry-U6-empty	Addgene	#140580
pmCherry-U6-EMX1	Addgene	#140581
pmCherry-U6-TTLL11	Addgene	#140582
pmCherry-U6-CLIC3	Addgene	#140583
pmCherry-U6-RNF103-CHMP3	Addgene	#140584
pmCherry-U6-RGS8	Addgene	#140585
pmCherry-U6-GTPBP2	Addgene	#140586
pmCherry-U6-SYNPO	Addgene	#140587
pmCherry-U6-VEGFA	Addgene	#140588
pmCherry-U6-ALDH1A3	Addgene	#140589
pmCherry-U6-CACNG3	Addgene	#140590
pTBX1-Tn5	Addgene	#60240
pX165	Addgene	#48137
pCMV-PE2	Addgene	#132775
pU6-pegRNA-GG-acceptor	Addgene	#132777
pX165-Sniper-Cas9	This study	N/A
pX165-LZ3 Cas9	This study	N/A
pX165-HiFi Cas9	This study	N/A
pX165-eSpCas9	This study	N/A
pX165-Cas9-HF1	This study	N/A
pX165-HypaCas9	This study	N/A
pX165-xCas9	This study	N/A
pX165-evoCas9	This study	N/A
Software and Algorithms		
BrowserGenome	http//BrowserGenome.org	N/A
OutKnocker	http://OutKnocker.org	N/A
Elevation scoring	https://crispr.ml	N/A
GuideScan	https://guidescan.com	N/A
FORECasT	https://partslab.sanger.ac.uk/FORECasT	N/A

Continued

REAGENT or RESOURCE	SOURCE	IDENTIFIER
inDelphi	https://indelphi.giffordlab.mit.edu/single	N/A
Lindel	https://github.com/shendurelab/Lindel	N/A
Other		
Bench Protocol	(this paper)	STAR Methods

LEAD CONTACT AND MATERIALS AVAILABILITY

Further information and requests for resources and reagents should be directed to and will be fulfilled by the Lead Contact, Feng Zhang (zhang@broadinstitute.org). Plasmids generated in this study have been deposited to Addgene.

EXPERIMENTAL MODEL AND SUBJECT DETAILS

HEK293T cells
HEK293T cells were maintained at 37C, 5% CO_2 in DMEM-GlutaMAX (GIBCO) supplemented with 10% FBS (Seradigm) and 10 μg/ml Ciprofloxacin (Sigma-Aldrich). HEK293T cells were originally derived from a female human embryo. Cells were obtained from the lab of Veit Hornung. Cell line authentication was not performed.

U-2 OS cells
U-2 OS cells were maintained at 37C, 5% CO_2 in DMEM-GlutaMAX (GIBCO) supplemented with 10% FBS (Seradigm) and 10 μg/ml Ciprofloxacin (Sigma-Aldrich). U-2 OS were originally established from the osteosarcoma of a female patient. Cells were obtained from ATCC. Cell line authentication was performed by the vendor.

K562 cells
K562 cells were maintained at 37C, 5% CO_2 in RPMI-GlutaMAX (GIBCO) supplemented with 10% FBS and 10 μg/ml Ciprofloxacin (Sigma-Aldrich). K562 cells were originally established from the chronic myelogenous leukemia of a female patient. Cells were obtained from Sigma-Aldrich. Cell line authentication was performed by the vendor.

E. coli strains
STBL3 *E. coli* cells (ThermoFisher) were grown in LB media at 37C overnight. Chemo-competent cells were generated using the Mix&Go kit (Zymo).

METHOD DETAILS

Tn5 purification
Tn5 was purified as previously described (Picelli et al., 2014). *E. coli* cells (NEB C3013) harboring pTBX1-Tn5 were grown in terrific broth to an OD of 0.65 before addition of IPTG at 0.25 mM. Protein expression was induced at 23°C overnight, and cells were harvested and stored at −80°C until purification. 20 g of *E. coli* pellet was lysed in 200 ml HEGX buffer (20 mM HEPES-KOH pH 7.2, 800 mM NaCl, 1 mM EDTA, 0.2% Triton, 10% glycerol) with cOmplete protease inhibitor (Roche) and 10 μl of benzonase (Sigma-Aldrich). Cells were lysed using a LM20 microfluidizer device (Microfluidics) and cleared by centrifugation at max speed for 30 min. 5.25 ml of 10% PEI (pH 7) was added dropwise to a stirring solution to remove *E. coli* DNA and the resulting precipitation removed after centrifugation for 10 min. Cleared supernatant was added to 30 ml of equilibrated chitin resin (NEB), mixed end-over-end for 30 min, added to column, washed with 1L HEGX buffer. 75 ml HEGX buffer with 100 mM DTT was added to column, 30 ml drawn through the resin before sealing the column and storing at 4°C for 48h to allow for intein cleavage and elution of free Tn5. Eluted Tn5 was dialyzed into 2xTn5 dialysis buffer (100 mM HEPES, 200 mM NaCl, 2 mM EDTA, 0.2 % Triton, 20% glycerol), with two exchanges of 1l of buffer. The final solution was concentrated to 50 mg/ml as determined by A280 absorbance (A280 1 = 0.616 mg/ml = 11.56 mM) and flash frozen in liquid nitrogen before storage at −80°C.

Tn5 loading with single handle
Oligonucleotides *Transposon ME* and *Transposon read 2* were annealed at a concentration of 42 μM each in annealing buffer (1.5 mM Tris-HCl pH 8.0, 150 μM EDTA, 30 mM NaCl) by heating to 95°C for 3 minutes, and subsequently ramping the temperature from 70°C to 25°C at a rate of 1°C per minute. 1 ml of purified Tn5 (50 mg/ml) were incubated with 355 μl of annealed oligonucleotides for 1 hour at room temperature. Of note, loaded Tn5 can crash out as white precipitate, but retains activity. Loaded Tn5 is stored at −20°C and ready to be thawed on ice for later use.

Cas9 variant cloning

Cas9 variants were cloned by site-directed mutagenesis into pX165 (Addgene #48137), which encodes a CBh promoter-driven SpCas9 containing a 3xFLAG tag and SV40 NLS on the N terminus and a nucleoplasmin NLS on the C terminus.

Cell transfection

HEK293T cells were seeded in poly-D-lysine coated 96-well plates (Corning) at a density of 25,000 cells in 100 μl medium per well. The next day, 250 μl OptiMEM (Thermo) were mixed with 1 μg of oligonucleotide donor (*TTISS donor sense* and *TTISS donor antisense*, annealed in 0.1x IDT Nuclease-Free Duplex Buffer by ramping the temperature from 95°C to 25°C at a rate of 1°C per minute), 750 ng Cas9 expression plasmid, and a total of 250 ng of 1-60 different gRNA expression plasmids (sequences in Table S3). In parallel, 250 μl OptiMEM were mixed with 5 μl GeneJuice (Millipore) and incubated at room temperature for 5 minutes. After mixing all components and incubating them for 20 minutes, 50 μl were added drop-wise per 96-well of cells in a total of ten wells per condition. For prime editing, the same transfection protocol was used with 1.5 μg pCMV-PE2 plasmid and 500 ng pU6-pegRNA. For TTISS in K562 and U-2 OS cells, one million cells were nucleofected with pulse code FF-120 (K562) or CM-104 (U-2 OS) using a Lonza 4D-Nucleofector X unit in 100 μl buffer SF (K562) or SE (U-2 OS) with the same amounts of Cas9, gRNA, and donor as listed above.

Cell lysis and genome tagmentation

Three days after transfection, cells were washed with PBS, trypsinized, and washed again in a 1.5 ml tube. Pelleted cells were lysed by re-suspending one million cells in 100 μl lysis buffer (1 mM $CaCl_2$, 3 mM $MgCl_2$, 1 mM EDTA, 1% Triton X-100, 10 mM Tris pH 7.5, 8 units/ml Proteinase K (NEB)) and heating to 65°C for 10 minutes. For tagmentation, 80 μl crude lysate were mixed with 25 μl 5x TAPS buffer (50 mM TAPS-NaOH pH 8.5 at room temperature, 25 mM $MgCl_2$) and 20 μl hyperactive loaded Tn5 transposase and were heated to 55°C for 10 minutes. Reactions were mixed with 625 μl PB buffer (QIAGEN) and purified on a mini-prep silica spin column according to the protocol (QIAGEN). DNA was eluted in 50 μl water (typical concentration: 200-300 ng/μl).

PCR amplification

Total eluates were denatured at 95°C for 5 minutes, snap-cooled on ice, and amplified in 200 μl PCR reactions using KOD Hot Start polymerase (Millipore) according to the manufacturer's protocol (12 cycles, Ta = 60°C, one minute elongation, primers: *TTISS PCR fwd 1*, *Transposon read 2*). For each sample, a secondary 50 μl KOD PCR was templated with 3 μl of the first PCR reaction and a unique barcoding primer (20 cycles, Ta = 65°C, one minute elongation, primers: *TTISS PCR fwd 2*, *TTISS PCR rev BC1-24*). For mapping prime-mediated insertions, primers *TTISS PCR prime +24 fwd a, b* or *TTISS PCR prime +38 fwd a1, a2, b1, b2* were used instead.

Deep sequencing

PCRs were pooled, column-purified, and 250-1,000 bp fragments were enriched using a 2% agarose gel. After two consecutive column purifications, the library was quantified using a NanoDrop spectrometer (Thermo) and sequenced using an Illumina NextSeq 500 sequencer with a 75-cycle high-output v2 kit (cycle numbers: read 1 = 59, index 1 = 8, read 2 = 25, no index 2).

Read mapping

Reads were mapped to human genome version *hg38* using https://BrowserGenome.org (Schmid-Burgk and Hornung, 2015) with mapping parameters: read filter = NNNNNNNNNNNNNNNNNNNNNNNNNAAC, forward mapping start = 26 bp, forward mapping length = 25 bp, reverse mapping length = 15 bp, max forward/reverse span = 1000 bp. For mapping prime-mediated insertions, read filters CTTATCGTCGTCATCCTTGTAATC (+24 a, forward mapping start = 25), GATTACAAGGATGACGACGATAAG (+24 b, forward mapping start = 25), GACGGCGGTCTCCGTCGTCAGGATCAT (+38 a, forward mapping start = 28), or GACGGAGACCGCCGTCGTCGACAAGCC (+38 b, forward mapping start = 28) were used instead. Mapped read pairs spanning fewer than 37 genome bases were discarded in order to omit signal from the pegRNA expression plasmid.

Integration site detection

Common break sites, common mispriming sites and reads mapping to the human U6 promoter were filtered out. These were detected by TTISS in the absence of a nuclease, donor, and/or gRNA plasmid. Following removal of non-overlapping single-read noise, putative break sites were identified by the presence of two or more unique reads mapping to the reference sequence within a window of 20 nucleotides. For all sites passing filters, TTISS read counts mapping to a 60-nucleotide window were tabulated and stored for downstream analysis.

gRNA assignment

For each 60-nucleotide window, peaks were identified in both the sense and antisense reads, and each peak was grouped with all gRNA sequences used in the respective experiment whose spacers had an edit distance less than or equal to 6 mismatches for any 20-mer in a window of 25 nucleotides on either side of the detected peak site. If a given peak site had at least one such gRNA, then a cut site score was calculated for each putative gRNA match. The cut site score was defined as the distance between the expected cut site of the spacer and the peak. Each remaining peak site was then assigned to gRNA with the lowest cut site score and all peak sites

with a cut site score of between −3 and 3 were retained and reported for each individual gRNA. This allows for the possibility of multiple cut sites within the same window, as well as for the removal of false hits where the apparent cut site does not line up with the expected cut site from the spacer sequence.

Prediction of indel length distributions

Genomic positions of TTISS-detected donor integration events were tabulated for each gRNA target site with more than 50 reads mapping in each orientation. Obtained distributions were normalized to their total number of reads in order to obtain two frequency distributions per target site. TTISS-predicted indel length distributions were calculated by numerically convolving the two directional distributions for each target site. From each indel length distribution, relative +1 frequencies were calculated as the ratio of +1 frequency to the sum of all non-+0 repair frequencies.

Variant Scoring

Specificity scores were calculated by subtracting from 100 the percent of TTISS reads that corresponds to off-targets. Activity scores were calculated as the mean indel percentage across all 59 on-target sites, normalized to WT SpCas9.

Cas9 variant library construction

SpCas9 variants were screened using a pool of self-targeting lentiviral vectors in which each lentiviral insert contained a Cas9 variant and a constant target site, allowing indel formation at the target site to be coupled to its corresponding Cas9 variant. For the variant pool, > 150 residue positions, concentrated in the HNH and RuvC nuclease domains, were selected for single amino acid saturation mutagenesis. For each residue, a mutagenic insert was synthesized as short complementary oligonucleotides, with the mutated codon replaced by a degenerate NNK mixture of bases, as previously described in Gao et al. (2017). Furthermore, variants were barcoded with a random 24-nt sequence placed in close proximity to the target site in order to allow direct variant-to-indel association by short-read paired-end sequencing. Barcode-to-variant associations were determined by targeted deep sequencing prior to performing the screen.

Lentiviral Cas9 variant library screen

HEK293FT cells were transduced with the variant library at MOI < 0.1 and selected with puromycin at 1 μg/ml over several passages to eliminate non-transduced cells. Variant library-transduced cells were subsequently transduced with a second lentivirus containing an U6-sgRNA expression cassette at MOI >> 1 and > 1000 cells/variant, in order to initiate indel formation at the target site. After approximately 4 days, genomic DNA from cells were isolated, and the target site and corresponding barcodes were PCR-amplified and paired-end sequenced with a 150-cycle NextSeq 500/550 High Output Kit v2 (Illumina). This procedure was repeated for four different sgRNAs: Two fully matched sgRNAs, to assess on-target efficiency of the variants; and two sgRNA bearing double base mismatches, to assess specificity (all guide sequences in Table S3). Highly abundant barcodes (above 50 reads; comprising 5%, 2%, 3% and 3% of all barcodes for g1, g2, g3 and g4, respectively) were discarded to reduce noise. For each guide, the score of a variant was calculated as 100 * (number of reads containing an indel) / (total number of reads pooled across all retained barcodes for that variant). Variants with fewer than 100 reads for any of the four target sites were discarded, resulting in a final set of 130 wild-type, 112 stop codons, and 2,420 single amino acid variants.

Cas9 variant validation and combinatorial mutagenesis

Top hits from the pooled variant screen that exhibited both high on-target efficiency and high specificity were individually cloned into pX165 (Ran et al., 2013) and tested at additional target sites in HEK293T cells, including sites that were previously observed to have substantially reduced activity with eSpCas9, SpCas9-HF1, and HypaCas9. Top-performing variants were combined to produce combination mutants, including LZ3 Cas9, which were re-tested as described and refined over 10 subsequent rounds of mutagenesis.

Prime editing constructs

pegRNA sequences were cloned into pU6-pegRNA-GG-acceptor according to the protocol described in Anzalone et al. (2019) (Table S3).

Targeted indel sequencing

Indel frequencies were quantified by targeted deep sequencing (Illumina) as previously described in Gao et al. (2017). Indel distribution profiles were analyzed using https://OutKnocker.org (Schmid-Burgk et al., 2014).

Indel distribution and specificity predictors

Elevation scores (Listgarten et al., 2018) and GuideScan (Perez et al., 2017) scores were calculated by inputting the gene into the online interfaces (https://crispr.ml and https://guidescan.com) and storing the Elevation aggregate value and specificity value for the correct gRNA respectively. Predicted +1 insertion frequencies from FORECasT (Allen et al., 2018) and inDelphi (Shen et al., 2018) were evaluated by inputting the genomic locus (FORECasT) or 30 bp on either side of the cut site (inDelphi) into the correct

CellPress

online interface (https://partslab.sanger.ac.uk/FORECasT and the HEK293 predictor on https://indelphi.giffordlab.mit.edu/single) and recording the total predicted % of 1-bp insertions. Lindel-predicted values (Chen et al., 2019) were calculated similarly to inDelphi using the Python library (https://github.com/shendurelab/Lindel).

QUANTIFICATION AND STATISTICAL ANALYSIS

The code used for sequencing data mapping used in this study is available at https://www.BrowserGenome.org. No data were excluded from analysis. Statistical tests and significance thresholds are indicated in the legends to Figure 3.

DATA AND CODE AVAILABILITY

The sequencing data generated during this study are available at SRA (SRA: PRJNA602092). The code used for read post-processing used in this study is available at GitHub (schmidburgk/TTISS).

ADDITIONAL RESOURCES

Detailed protocol
A detailed bench protocol describes the experimental details of the TTISS method.

Bench Protocol
Step 1: Tn5 purification
- Grow *E. coli* cells (NEB C3013) harboring the plasmid pTBX1-Tn5 in terrific broth to an OD of 0.65
- Add IPTG to a concentration of 0.25 mM and shake at 23°C overnight
- Harvest cells by centrifugation and store at −80°C until purification
- Lyse 20 g of *E. coli* pellet in 200 ml HEGX buffer (20 mM HEPES-KOH pH 7.2, 800 mM NaCl, 1 mM EDTA, 0.2% Triton, 10% glycerol) with cOmplete protease inhibitor (Roche) and 10 μl of Benzonase (Sigma-Aldrich), using an LM20 microfluidizer device (Microfluidics)
- Clear the lysate by centrifugation at max speed for 30 min
- Add 5.25 ml of 10% PEI (pH 7) dropwise to a stirring solution to remove *E. coli* DNA. for 10 min
- Add cleared supernatant to 30 ml of equilibrated chitin resin (NEB) and mix end-over-end for 30 min
  Add mixture to column, wash with 1L HEGX buffer
- Add 75 ml HEGX buffer with 100 mM DTT to column, draw 30 ml through the resin before sealing the column and storing at 4°C for 48h to allow for intein cleavage and elution of free Tn5 Dialyze eluted Tn5 into 2xTn5 dialysis buffer (100 mM HEPES, 200 mM NaCl, 2 mM EDTA, 0.2 % Triton, 20% glycerol), with two exchanges of 1l of buffer
- Concentrate the final solution to 50 mg/ml as determined by A280 absorbance (A280 1 = 0.616 mg/ml = 11.56 mM)
  Flash-freeze in liquid nitrogen before storage at −80°C
  Step 2: Tn5 loading with single handle
- Anneal oligonucleotides Transposon ME and Transposon read 2 at a concentration of 42 μM each in annealing buffer (1.5 mM Tris-HCl pH 8.0, 150 μM EDTA, 30 mM NaCl) by heating to 95°C for 3 minutes, and subsequently ramping the temperature from 70°C to 25°C at a rate of 1°C per minute
- Incubate 1 ml of purified Tn5 (50 mg/ml) with 355 μl of annealed oligonucleotides for 1 hour at room temperature. Of note, loaded Tn5 can crash out as white precipitate, but retains activity. Store loaded Tn5 at −20C, ready to be thawed on ice for later use. Resuspend before use.
  Step 3: Cell transfection
- Seed HEK293T cells in poly-D-lysine coated 96-well plates (Corning) at a density of 25,000 cells in 100 μl medium per well
- Anneal TTISS donor sense and TTISS donor antisense in 0.1x IDT Nuclease-Free Duplex Buffer by ramping the temperature from 95°C to 25°C at a rate of 1°C per minute
- The next day, mix 250 μl OptiMEM (Thermo) with 1 μg of annealed oligonucleotide donor, 750 ng Cas9 expression plasmid, and a total of 250 ng of 1-60 different gRNA expression plasmids for each condition
- In parallel, mix 250 μl OptiMEM with 5 μl GeneJuice (Millipore) and incubate at room temperature for 5 minutes for each condition
- Mix all components for each condition and incubate them for 20 minutes
- Add 50 μl drop-wise per 96-well of cells in a total of ten wells per condition
  Step 4: Cell lysis and genome tagmentation
- Two to three days after transfection, wash cells with PBS, trypsinize, and wash again with PBS in a 1.5 ml tube
- Lyse pelleted cells by re-suspending one million cells in 100 μl lysis buffer (1 mM CaCl2, 3 mM MgCl2, 1 mM EDTA, 1% Triton X-100, 10 mM Tris pH 7.5, 8 units/ml Proteinase K (NEB))
- Heat lysates to 65°C for 10 minutes, then keep on ice

- For tagmentation, mix 80 μl crude lysate with 25 μl 5x TAPS buffer (50 mM TAPS-NaOH pH 8.5 at room temperature, 25 mM MgCl2) and 20 μl hyperactive loaded Tn5 transposase. Heat to 55°C for 10 minutes.
- Mix reactions with 625 μl PB buffer (QIAGEN) and bind to a mini-prep silica spin column. Wash with 750 μl buffer PE (QIAGEN), spin dry, and elute DNA in 50 μl water (typical concentration: 200-300 ng/μl).
- Run 3μl of the eluate on a 2% Agarose gel to check size range If size range is outside the range of 300 to 1,000 bp, repeat with adjusted amounts of Tn5 and note adjustments for future use of the Tn5 batch. Alternatively, you can perform a titration of loaded Tn5 at the start using extra cell lysate to determine optimal tagmentation conditions.

Step 5: PCR amplification

- Denature total eluates at 95°C for 5 minutes, then snap-cool on ice
- Amplify in 200 μl PCR reactions using KOD Hot Start polymerase (Millipore) according to the manufacturer's protocol (12 cycles, Ta = 60°C, one minute elongation, primers: TTISS PCR fwd 1, Transposon read 2)
- For each sample, perform a secondary 50 μl KOD PCR templated with 3 μl of the first PCR reaction and a unique barcoding primer (20 cycles, Ta = 65°C, one minute elongation, primers: TTISS PCR fwd 2, TTISS PCR rev BC1-24)

Step 6: Deep sequencing

- Pool PCRs on ice, column-purify on a mini-prep silica column, and purify fragments within a size range of 250-1,000 bp using a 2% agarose gel
- Perform two consecutive column purifications (first with buffer QG (QIAGEN) and isopropanol added to the gel slice before loading, second with buffer PB and the eluate from the previous column)
  Quantify the library using a NanoDrop spectrometer (Thermo)
- Sequence using an Illumina NextSeq 500 sequencer with a 75-cycle high-output v2 kit (cycle numbers: read 1 = 59, index 1 = 8, read 2 = 25, no index 2)

Step 7: Read mapping

- Open in a web browser the site http://www.BrowserGenome.org
- Click the ''Map deep sequencing data'' tab
- Under point 2 click "Browse" to choose the human genome file "hg38.2bit" on your hard drive (download from http://hgdownload.cse.ucsc.edu/goldenPath/hg38/bigZips/hg38.2bit)
- Under point 3 click "Browse" to choose all un-compressed FASTQ files to be analyzed
- Under point 4, enter the filter values 0 bp, NNNNNNNNNNNNNNNNNNNNNNNAAC
- Under point 5 enter forward mapping start = 26 bp
- Under point 6 enter forward mapping length = 25 bp
- Under point 7 enter reverse mapping length = 15 bp
- Under point 8 enter max forward/reverse span = 1000 bp
- Click "Start mapping," which takes about one hour per ten million reads
- When all data has been processed, click "Save all" on bottom right to save mapping data files
- Click on the "Process" tab, then "Remove single read noise" and "Enforce antisense-overlap reads" for basic noise reduction and off-target site identification
- Click "Export peak list" to save a list of detected cleavage sites, which can be opened in a text or spreadsheet editor for further analysis
- For more complex analyses (such as gRNA multiplexing or indel distribution prediction), refer to the Read Me on the Github repository available at https://github.com/schmidburgk/ttiss